



This is a repository copy of *The Scoraig wind trials – in situ power performance measurements of locally manufactured small wind turbines.*

White Rose Research Online URL for this paper:
<https://eprints.whiterose.ac.uk/162396/>

Version: Published Version

Article:

Leary, J., Piggott, H. and Howell, R. orcid.org/0000-0002-0142-9728 (2021) The Scoraig wind trials – in situ power performance measurements of locally manufactured small wind turbines. *Wind Engineering*, 45 (3). pp. 727-749. ISSN 0309-524X

<https://doi.org/10.1177/0309524X20932501>

Reuse

This article is distributed under the terms of the Creative Commons Attribution (CC BY) licence. This licence allows you to distribute, remix, tweak, and build upon the work, even commercially, as long as you credit the authors for the original work. More information and the full terms of the licence here:
<https://creativecommons.org/licenses/>

Takedown

If you consider content in White Rose Research Online to be in breach of UK law, please notify us by emailing eprints@whiterose.ac.uk including the URL of the record and the reason for the withdrawal request.



eprints@whiterose.ac.uk
<https://eprints.whiterose.ac.uk/>

The Scoraig wind trials – In situ power performance measurements of locally manufactured small wind turbines

Wind Engineering
2021, Vol. 45(3) 727–749
© The Author(s) 2020



Article reuse guidelines:

sagepub.com/journals-permissions

DOI: 10.1177/0309524X20932501

journals.sagepub.com/home/wie



Jon Leary^{1,2} , Hugh Piggott³ and Robert Howell¹

Abstract

This article presents new insight into the real-world performance of a range of open source locally manufactured small wind turbines designed to enable sustainable rural electrification. The power performance of seven machines was measured in situ and compared to wind tunnel, test site and other in situ data to produce a set of generic power curves. This article shows that the shape and size of the curve (and therefore the energy that will be generated) varies considerably. However, over-performance was just as likely as under-performance, validating the designer's predicted energy yields. Nonetheless, optimising the power curve by tuning the small wind turbine increased energy yields by up to 156%. Developing low-cost practical tools that can enable rapid power curve measurements in the field could help reduce uncertainty when planning rural electrification programmes and ensure that small wind turbines are able to deliver vital energy services in off-grid regions of developing countries.

Keywords

Power curve, small wind turbine, rural electrification, in situ testing, performance verification

Introduction

In the right context, the local manufacture of small wind turbines (SWTs) can make a valuable contribution to sustainable rural electrification (Batchelor et al., 1999; Eales et al., 2016; Leary et al., 2018, 2019; Sumanik-Leary et al., 2013). Globally 840 million people still do not have access to electricity at home (SE4All, 2017). SWTs can be produced with the skills and materials available in many developing country contexts, enabling distributed manufacture of low-cost off-grid power systems (Clausen et al., 2009; Ferrer-Martí et al., 2010; Ghimire et al., 2010; Latoufis et al., 2012; Peterson and Clausen, 2004). The wind turbine, described by Hugh Piggott of Scoraig Wind Electric and presented in *A Wind Turbine Recipe Book* (Piggott, 2013), is a rugged machine designed to be manufactured using only basic tools and techniques (see Figure 1). The success of this manual has permitted the dissemination of the technology across the world, with more than 1000 machines produced in over 25 countries (Site Expérimental pour le Petit Eolien National, 2013).

The design is open source and manufactured by hand, so every machine is slightly different. Some readers make purposeful modifications to the design, with the aim of optimising it for their local environmental conditions, or for the tools, techniques and materials available in their local context. Others will follow the manual step by step; however, hand manufacturing still introduces variation in the final product, which can affect power performance.

The predictability of solar power systems has contributed strongly to their now almost ubiquitous presence in rural electrification programmes across the Global South. Predicting how much energy will be available to future

¹Department of Mechanical Engineering, The University of Sheffield, Sheffield, UK

²Department of Geography, Loughborough University, Loughborough, UK

³Scoraig Wind Electric, Dundonnell, UK

Corresponding author:

Jon Leary, Department of Geography, Loughborough University, Epinal Way, Loughborough LE11 3TU, UK.

Emails: j.leary@lboro.ac.uk; jonkleary@gmail.com

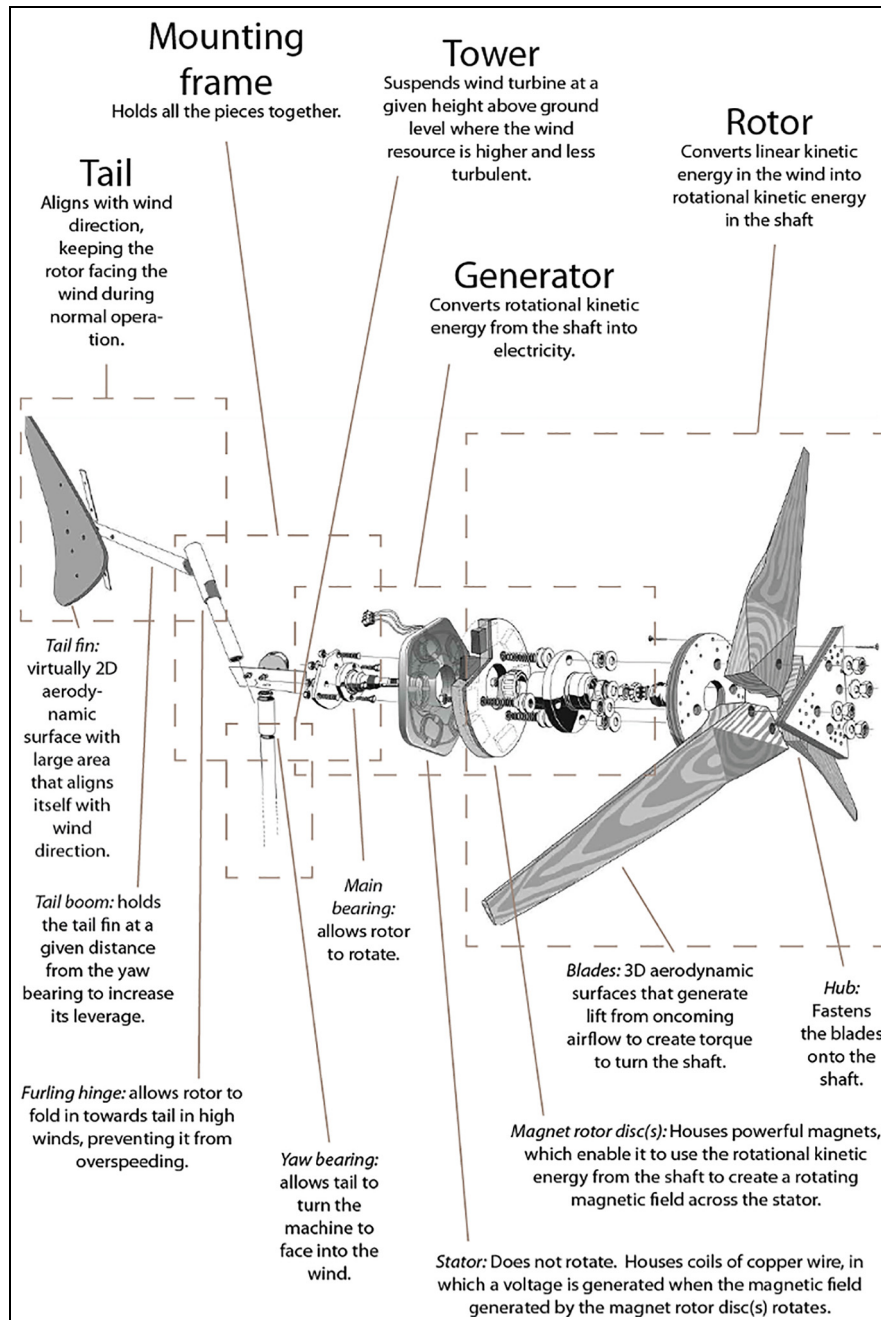


Figure 1. Annotated exploded CAD illustration of the major components of a Piggott turbine. Underlying CAD image courtesy of Roland Beile and Réseau Triपालium.

users of renewable energy systems greatly increases the scalability of rural electrification initiatives. However, small-scale wind power has many more uncertainties than solar (Leary et al., 2018).

Fundamentally, the wind resource is much more variable (in both space and time) than the sun, and a SWT is much more unpredictable than a solar panel. Maintenance is a well-known challenge with SWTs (Carvalho Neves et al., 2015; Leary et al., 2012, 2019); however, several studies have also highlighted the inconsistencies between power performance data provided by manufacturers with what is measured in the field, especially on high-turbulence sites (Encraft, 2009; Ingreenious, 2010; Medd and Wood, 2018). In particular, the Warwick Wind Trials (Encraft, 2009) exposed the exaggerations made by manufacturers and the weaknesses of the machines available on the UK market at that time. Locally manufactured machines, each of which is slightly different, could

be expected to exhibit even greater variation, which is a hypothesis put to the test by this study that offers valuable real-world data on a sector that has until now been poorly monitored.

When planning rural electrification programmes, the power curve of each model of SWT is usually assumed to be consistent. However, in reality, this article shows that it depends on many factors, such as the installation site, the age of the SWT, how well it has been maintained and the quality of manufacturing. Underperforming machines are often not identified as such until years after their installation, when disappointing energy yields limit the use of energy services, often resulting in SWTs being replaced by solar panels (Carvalho Neves et al., 2015).

Aims and objectives

The aim of this study is to gain new insight into the real-world performance of Piggott's open-source SWTs by measuring and comparing the performance of a range of machines in situ.

The objectives are as follows:

- To take a snapshot of the performance of the specific machines under test on the particular sites on which they are currently installed.
- To analyse this data set to determine the factors that most greatly affect power performance of locally manufactured SWTs.
- To compare the measured performance data with data from other studies and Piggott's design values to produce a generic set of power curves that represent the real-world performance of these machines.

Literature review

Piggott (2013)'s construction manual contains estimates for energy yields; however, few accurate performance measurements have been made. Even fewer relate directly to the machines described in the manual, as modifications are often made to the core design. Table 1 compares and contrasts other measurement campaigns for Piggott's SWTs.

Four organisations carried out power curve testing at unaccredited test sites. Chevalier tested a 1.8 N and 2.4 N against a range of other commercial turbines at the Schoondijke test site in the Netherlands (Ingreenious, 2010); however, a single anemometer was used for all SWTs and power curves were produced from 5-min averages of energy yield.¹ Quéval et al. (2014) measured a 3.6 m diameter neodymium machine at a test site in Nicaragua; however, the SWT was modified for the low wind speeds characteristic of the Caribbean coast (Piggott, 2013). Chiroque et al. (2008) and Sánchez et al. (2002) measured the performance of both 1.7 m and 3 m machines that had evolved from Piggott's early designs both before and after upgrading from ferrite to neodymium magnets; however, the data set was limited and the measurement procedure unknown. Finally, Latoufis et al. also used the IEC 61400-12-1 standard as a guide to test a 2.4 N at the National Technical University of Athens (NTUA) test site in Rafina, Greece (Latoufis et al., 2014).

Two organisations have tested Piggott's SWTs at nationally accredited test sites. A 2.4 m machine based on Piggott's design was tested by National Industrial Technology Institute (INTI) Neuquén in Cutral-Có, Argentina (INTI, 2016). Eolocal altered the design to industrialise the manufacturing process; however, the parts are interchangeable with standard Piggott machines, so the performance should be similar and in theory, more consistent. A 3.6 m turbine built by Ti'eole was measured at the French national small wind test site (Site Expérimental pour le Petit Eolien National, 2013); however, this machine was grid-connected, which significantly increases the performance, as tip speed and load voltages are decoupled.

Two organisations used wind tunnel testing to explore power performance under controlled conditions. Monteiro et al. (2013) characterised the rotor performance of a 1.2 N built by Ti'eole in the Associação para o Desenvolvimento da Aerodinâmica Industrial² wind tunnel in Portugal. Hosman (2012) tested both the rotor and generator of a 1.8 N in the TU Delft wind tunnel in the Netherlands. Wind tunnel tests allow for close inspection of aerodynamic performance under controlled conditions; however, real wind is not controlled – gusts and direction changes make real wind turbine performance much more dynamic.

Finally, Dotan (2017). also carried out in situ field measurements to optimise the performance of seven SWTs manufactured by Community Energy and Technology in the Middle East (COMET-ME) in Palestine. However, data were not filtered by wind direction and several of the curves seem unexpectedly close to the Betz limit (see Figure 8).

Table I. Comparison of the literature on performance testing of *Recipe Book* (Piggott, 2013) designs.

Publication	Turbine	Tester	Location	SWT diameter	Major modifications from Recipe Book	Test procedure and site description
Chiroque et al. (2008), Sánchez et al. (2002)	SP-500	Soluciones Prácticas	Peru	3 m	PVC blades, generator reconfigured. Ferrite magnets on SP-100 upgraded to NdFeB.	Unknown.
Quéval et al. (2014)	SP-100 blueDiamond 3-TSR6	blueEnergy	Bluefields, Nicaragua	1.7 m 3 m	Bigger rotor	IEC 61400-12-1 as a guide. Ohio Semitronics current/voltage transducers, NRG Max40 anemometer, NRG 200P vane, Campbell CR10X logger. Filtered out 0 m/s, 0A; $\pm 5\% V_{\text{nominal}}$. Sea level pressure correction. IEC 61400-12-1 as a guide. Coastal cliff-top site but filtered by wind direction. LEM LV 25-P voltage and Honeywell CSNR151 current transducers. NRG 40C anemometer and NRG 200P wind vane. NRG-110 temp., NRG-BP-20 pressure and NRG-RH-5 humidity sensors. National Instruments NI6225 data acquisition card.
Latoufis et al. (2015)	NTUA 2.4 N	NTUA	NTUA Test Site, Rafina, Greece	2.4 m	None	IEC 61400-12-1 certified. National test site. Equipment unknown.
Zuliani (2013)	Ti'eole 3.6 N	Tripalium	Malbouissou, France	3.6 m	Grid connected	IEC 61400-12-1 certified. Equipment unknown.
INTI (2016)	Eolocal AG700	INTI	INTI Test Site, Cultral-Co, Argentina	2.4 m	Optimised for higher volume production, for example, fibreglass blades	IEC 61400-12-1 certified. Equipment unknown.

(continued)

Table I. Continued

Publication	Turbine	Tester	Location	SWT diameter	Major modifications from Recipe Book	Test procedure and site description
Raw data only	3 N	COMET-ME	Asfai, Palestine	3 m	Unknown	Procedure unknown. Data unfiltered. $P = 0$ W at $V > 4$ m/s filtered out. Logic Energy LeNet datalogger, other equipment unknown. No wind direction at Heribat a nabi – hillside with high turbulence.
	4.2 N		COMET-ME Centre, Palestine	4.2 m	15 coil, 20-pole generator	
	3 N			3 m	15 coil, 20 pole, 350 mm diameter rotor	
	3 N		Heribat a nabi, Palestine	3 m	Unknown	
	4.2 N		Shaeb Al Buttum, Palestine	4.2 m	Unknown	
	3 N		Tuba, Palestine	3 m		
Hosman (2012)	I Love Wind Power 1.8 N	TU Delft	Delft, Netherlands	1.8 m	None	Incrementally load rotor with prony brake or rotor/generator with dummy load to find equilibrium for each wind speed. Digital hand tachometer, transmissive optical sensor, loadcell, potentiometers, AC/DC current clamp, digital scale.
Monteiro et al. (2013)	Ti'eoie 1.2 N	University of Beira Interior	Coimbra, Portugal	1.2 m	Rotor only	Rotor tested by loading at constant wind speeds with electric motor. Pitot tube, TESTO 4800 optical rotational speed sensor, digital scale, rheostat.
Ingreenious (2010)	ILWP 2.4 N ILWP 1.8 N	Ingreeniuos	Schoondijke, Netherlands	2.4 m 1.8 m	None	Seven SWTs in a row, one anemometer, data not filtered by direction. $P = 0$ W at $V > 6$ m/s filtered out.

SWT: small wind turbine; NTUA: National Technical University of Athens; INTI: National Industrial Technology Institute; PVC: PolyVinyl Chloride; P: Power.

Table 2. The series of SWTs described by Piggott in his *Recipe Books* (Piggott, 2009, 2013), the preceding *How to Build a Wind Turbine* (Piggott, 2005) and local adaptations published by Wind Empowerment members (blueEnergy, 2009; Tripalium, 2017).

Model	Rotor diameter	Magnetic material	Construction manuals	Tested during this research
1.2 N	1.2 m	Neodymium	Piggott (2005, 2009, 2013), Tripalium (2017)	0
1.8 N	1.8 m	Neodymium	Piggott (2005, 2009, 2013), Tripalium (2017)	1 – 2009
2 F	2 m	Ferrite	Piggott (2014)	1 – 2014
2.4 N	2.4 m	Neodymium	Piggott (2005, 2009, 2013), Tripalium (2017)	3 – 2009
3 N	3 m	Neodymium	Piggott (2005, 2009, 2013), Tripalium (2017)	2 – 2009
3.6 N	3.6 m	Neodymium	Piggott (2005, 2009, 2013), Tripalium (2017)	0
4.2 N	4.2 m	Neodymium	Piggott (2005, 2009, 2013), Tripalium (2017), blueEnergy (2009)	0

In situ testing offers the most realistic but least controlled conditions. This study attempts to bring the repeatability of the techniques employed at test sites to in situ testing using the IEC 61400-12-1 standard as a guide. By measuring a series of wind turbines, each one of which was either built by Piggott, or in workshops under his supervision, to his *Recipe Book* specification (see Table 2), it is hoped that broader conclusions can be drawn regarding the factors that influence power performance.

Methodology

The international standard for power curve testing of SWTs, IEC-61400-12-1, guided the development of a practical, yet accurate and repeatable measurement procedure. The standard was developed for large-scale wind turbines, with an appendix detailing adaptations for SWTs to facilitate repeatability in measurements between internationally accredited SWT test sites. As a result, some of the suggested procedures are impractical to implement for in situ measurements and a simplified procedure was adopted if the impact on the power performance measurements was expected to be negligible.

Measurement system

This measurement campaign took place at Scoraig, Ross Shire, Scotland. A single measurement system was rotated around each individual site; however, due to the differences between turbines (e.g. AC vs DC power transmission) and sites (e.g. distance from turbine to battery bank), the measurement equipment varied slightly for each test. Figure 2 shows one particular configuration, while Table 3 describes the range of sensors, the datalogger and its power supply methods. The Logic Energy LeNet recorded data from sensors for wind speed and direction, current, voltage, rotational speed and temperature. Using the values for the accuracy of the datalogger and sensors in Table 3, the uncertainties for the most critical variables were estimated at $\pm 2\%$ for the power measurements and $\pm 5\%$ for the wind speed measurements. Data from each sensor were sampled at a rate of 1 Hz and averaged at 10-min intervals.³ Each set of 10-min averaged data was then written to an SD card and transmitted to the Logic Energy server (LeSense) over the Global System for Mobile Communications (GSM) network, where it could later be downloaded in .csv format for analysis.

Turbines

Table 5 shows the key mechanical and electrical characteristics of the seven turbines, indicating that there is significant variation between all parameters, but most notably:

- Blade geometry: initially due to hand carving and subsequently due to warping (altering pitch) and erosion of the leading edges.
- Generator: nominal voltage is a design parameter, matched to each household energy system voltage. In contrast, while the air gap has recommended values, it should be tuned on installation to accommodate some of the variability in hand manufacturing and balance reliability with power performance.⁴ Neodymium had superseded ferrite as the magnetic material of choice due to its far superior flux density. However, long supply chains, unstable prices, susceptibility to corrosion and the environmental impact of

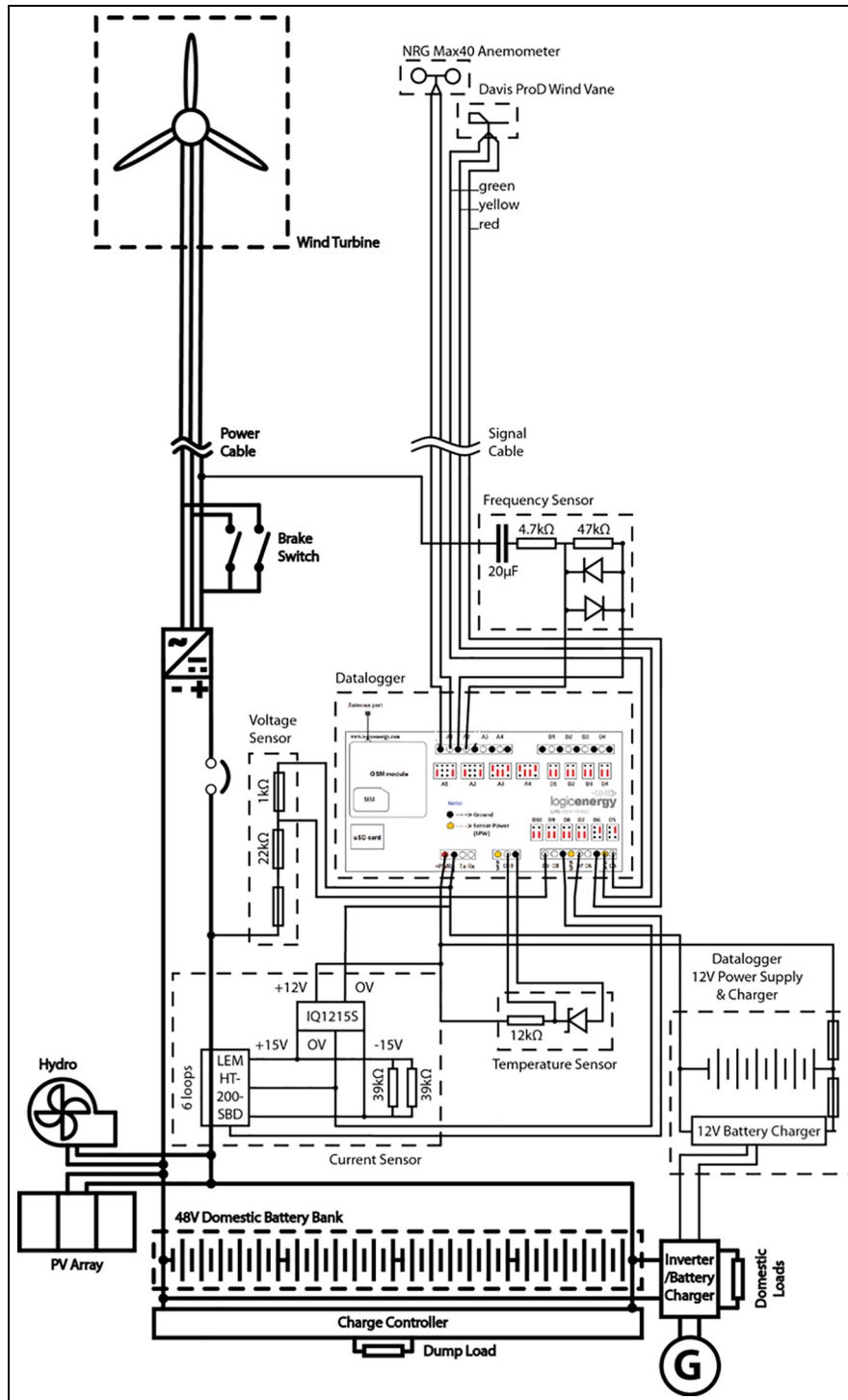


Figure 2. Wiring diagram showing the measurement sensors, datalogger and power supplies used during this measurement campaign. This diagram is from Site E; variations between sites are summarised in Table 4 and the resultant adaptations made to the measurement set up are listed in Table 3.

this rare earth metal have renewed interest in ferrite, particularly for coastal locations where corrosion is often extreme.

- Furling: there are also recommended values for tail moments, but it should also be tuned on installation to balance out the individual machine’s characteristics, the influence of each site and the users’ preferences.⁵

Table 3. Variables measured during this measurement campaign and specifications of sensing, power supply and datalogger equipment used to measure/record them modules.

Variable/component	Sensor/component type	Digital (pulse count) or analog	Brand/Model	Description
Wind speed	Anemometer	Digital	(a) NRG Max40 (± 0.14 m/s) (b) Second Wind C3 (± 0.1 m/s)	Mounted on separate met mast 2–4 rotor diameters from the SWT. Anemometer mounted at $\pm 10\%$ of hub height. ^a
Wind direction	Wind vane	Analog	(a) Davis Pro-D ($\pm 3^\circ$) (b) Inspeed E-vane ($\pm 1.8^\circ$)	Mounted on boom on same met mast.
Rotational speed	AC frequency	Digital		Raw signal transformed into countable pulses by capacitor, diodes and potential divider.
Current	Hall effect	Analog	(a) LEM HT200-SRUD ($\pm 1\%$) (b) Multicomp TMA100A ($\pm 1\%$)	Range varied by looping power cable through sensor.
Voltage	Direct measurement	Analog		Configurations: a) Direct measurement from input voltage (12 V systems) b) Potential divider (24/48 V systems)
Temperature	Zener diode	Analog		Potential divider controlled by Zener diode – resistance proportional to temperature. ^b
Pressure	Not measured			All sites below 100 masl, so adjustment of air density likely to be minimal.
Datalogger	Multichannel datalogger: • Eight digital pulse inputs • Six analog ports		Logic Energy LeNet (digital inputs: $\pm 0.01\%$, analog inputs: $\pm 0.5\%$)	Data recorded on SD card and transmitted through GSM network to LeSense cloud platform: • 1 Hz sampling • 10-min averaging (max., avg. and SD stored) Power supply configurations: a) Remote logging (dedicated battery) b) Domestic battery charging (dedicated battery charging from SWT battery bank) c) Direct connection (to SWT battery bank)

SWT: small wind turbine; GSM: Global System for Mobile Communications.

^aIEC 61400-12-1 specifies $\pm 2.5\%$.

^bTemperature measured at logger, not on met mast as specified by IEC 61400-12-1.

Turbine G was measured twice: before and after converting to a *Recipe Book* machine. The turbine had originally been built with a 12 V *Jerry-rigged*⁶ stator to investigate the viability of this alternative configuration. However, very poor results from the first measurement campaign (G-I) inspired the upgrading of the stator to a standard *Recipe Book* 24 V configuration, repainting of the blades and the shortening of the tail boom. The measurement set up was left in place and another data set (G-II) was measured immediately after.⁷

Sites

The aim of IEC-61400-12-1 is to offer a repeatable test procedure that will yield identical results on every site. However, it is inevitable that if any one of the seven turbines were tested across all of the seven sites, then the performance curve measured on each would be slightly different, even after all ‘invalid’ data had been excluded. For

example, the turbulence introduced by far away trees or mountains, the length of the power cable and the loading provided by the battery bank and dump load all influence the measured performance, even when within the guidelines set by IEC-61400-12-1.

Table 4 categorises the main factors that are likely to influence performance on a specific site and compares between the seven test sites in this study. Figure 3 shows where each of the test sites is located on the Scoraig peninsula, giving an indication of the range of surrounding topographies and vegetation. Sites A, B and F are all exposed hillsides above the main settlement on the southern side of the peninsula, trading off long power cables for better wind resource. Sites C, E and G are closer to the households they supply but nestled within the scattered trees and hedgerows of the settlement, creating significant turbulence. Site D is on the Northern side of the peninsula, with high turbulence at various length scales created by both the nearby trees and house, as well as the hillside and mountain. Site B is the only 100% wind system, meaning that the battery voltage and therefore the power performance are dictated purely by the current wind conditions and load. The systems at Sites A, D and G are renewable-only PV-wind systems, with the remainder backed up by generators. The systems at Sites F, B and D have lower cost design philosophies, while those at Sites E and C prioritise reliability.

Data processing

Data were downloaded in .csv format from the LeSense and processed using Excel and Matlab (see Figure 4). In addition to the steps specified by IEC-61400-12-1, Table 6 summarises the additional data verification carried out to identify, then correct or exclude invalid data caused by faulty sensors, power generation equipment and/or unavoidable user behaviour. The amount of data recorded at each site varied significantly, primarily due to the frequency of storms required to fill up the higher wind speed bins.

Results

Figure 5 shows a huge variation in normalised power performance, especially once the furling system is active. Figure 6 shows the implication of this on energy yields, with some machines underperforming and some overperforming compared to Piggott's predictions. The strong furling systems of E, F, G-I and B clearly limit energy yields on higher wind sites, prioritising robustness over power performance. There is little correlation between rotor size and normalised power performance, indicating that bigger machines are not necessarily more efficient. Data set G indicates the importance of post-installation performance evaluation and fine-tuning, as this machine was upgraded from the worst performing to the best.

Discussion

Key factors affecting power performance

Detailed analysis of the individual data sets and comparing between them identified several factors that influence the power performance of locally manufactured SWTs. Unfortunately, without further data collection, it is not possible to say how much influence each factor has. This could be achieved by identifying the most likely causes of diminished performance on each machine, carrying out appropriate corrective action, then remeasuring the power curve to quantify the increase in performance. This procedure was carried out on Site G, resulting in a 70% increase in energy yield on low wind sites (3 m/s annual mean) and a 156% increase on high wind sites (7 m/s annual mean). However, as three upgrades were made to the machine simultaneously (tail boom lengthened, stator switched for 24 V delta, blades repainted), it was not possible to assess the influence of each modification individually.

Main power-generating region. In the main power-generating region (4–8 m/s), blade performance and air gap were expected to have the biggest influence on power performance; however, no correlation with either factor was observed. In theory, a smaller air gap improves efficiency by increasing flux density; however, previous trial and error experimentation during the design of the *Recipe Book machines* suggested that the tuning of the machine's speed (volts/RPM) has a *sweet spot* that offers an acceptable tip speed ratio over the whole range of wind speeds. This can be tweaked using the air gap; if the gap is too small, then the low RPM can lead to stalling of the rotor at low battery voltage, which dramatically reduces performance as wind rises.

Table 4. Technical description of the sites where the seven turbines were located during this measurement campaign.

Tower	Power cable ^a	Major obstructions ^b	Roughness (valid sections only)	Other power generation sources	Battery bank	Slope	Key observations
A	7.7 m 67 m 0.19 Ω DC	House (50 m from SWT)	Heather and rocks (0.1)	180 W PV	12 V, 400Ah	Evenly sloping towards Southwest	Small PV-wind hybrid system on an exposed hillside.
B	7.7 m 183 m 0.69 Ω DC	3.6 m SWT diameter operating 30 m away	Heather and rocks (0.1)	n/a	24 V, 1240Ah	Gentle Southwest slope, leading onto much steeper slope	Good site on exposed hillside, but very long power cable. Big battery bank as no other generation sources.
C	10.5 m 52 m 0.20 Ω AC	House and trees (20–35 m from SWT)	Bushes (0.5)	Ampair Hawk (100 W) 588 W PV 6 kW generator	12 V, 800Ah	Gentle Southwest slope	PV-wind hybrid system with generator backup built for reliability. Reasonably clear site in predominant wind direction.
D	10 m 40 m 0.22 Ω AC	House and trees (5–25 m from SWT)	Bushes (0.5)	628 W PV	24 V, 1600Ah	Gentle Northerly slope, much steeper either side	Most complex site: high turbulence from mountain and nearby house/trees. Low-cost PV-wind hybrid with big battery bank as no generator backup.
E	12 m 62 m 0.58 Ω AC	Small wood around house 20–50 m from SWT	Bushes (0.5)	320 W PV 100 W hydro 6 kW generator	48 V, 400Ah	Southeasterly slope	PV-hydro-wind-diesel hybrid built for reliability. High tower for complex site with many obstructions.
F	7.5 m 150 m 0.33 Ω DC	<1 m diameter SWT on 5 m tower 10 m away	Heather and rocks (0.1)	–200 W PV –500 W generator	24 V, 600Ah	Gentle Southwest slope, leading onto much steeper slope	Low-cost PV-wind hybrid. Good wind site on exposed hillside with long but low resistance power cable.
G	12 m 40 m 0.28 Ω AC	High row of trees and trees clumped around house 40 m away	Bushes (0.5)	–180 W upgraded to 240 W PV	12 V, 600Ah upgraded to 24 V, 800Ah	Evenly sloping towards Southwest	High tower for semi-open site. PV and battery bank upgraded between first and second measurement campaigns

SWT: small wind turbine.

^aUnless otherwise stated, power cable length and therefore resistance is from tower top to battery bank.

^bData from these sectors were excluded.

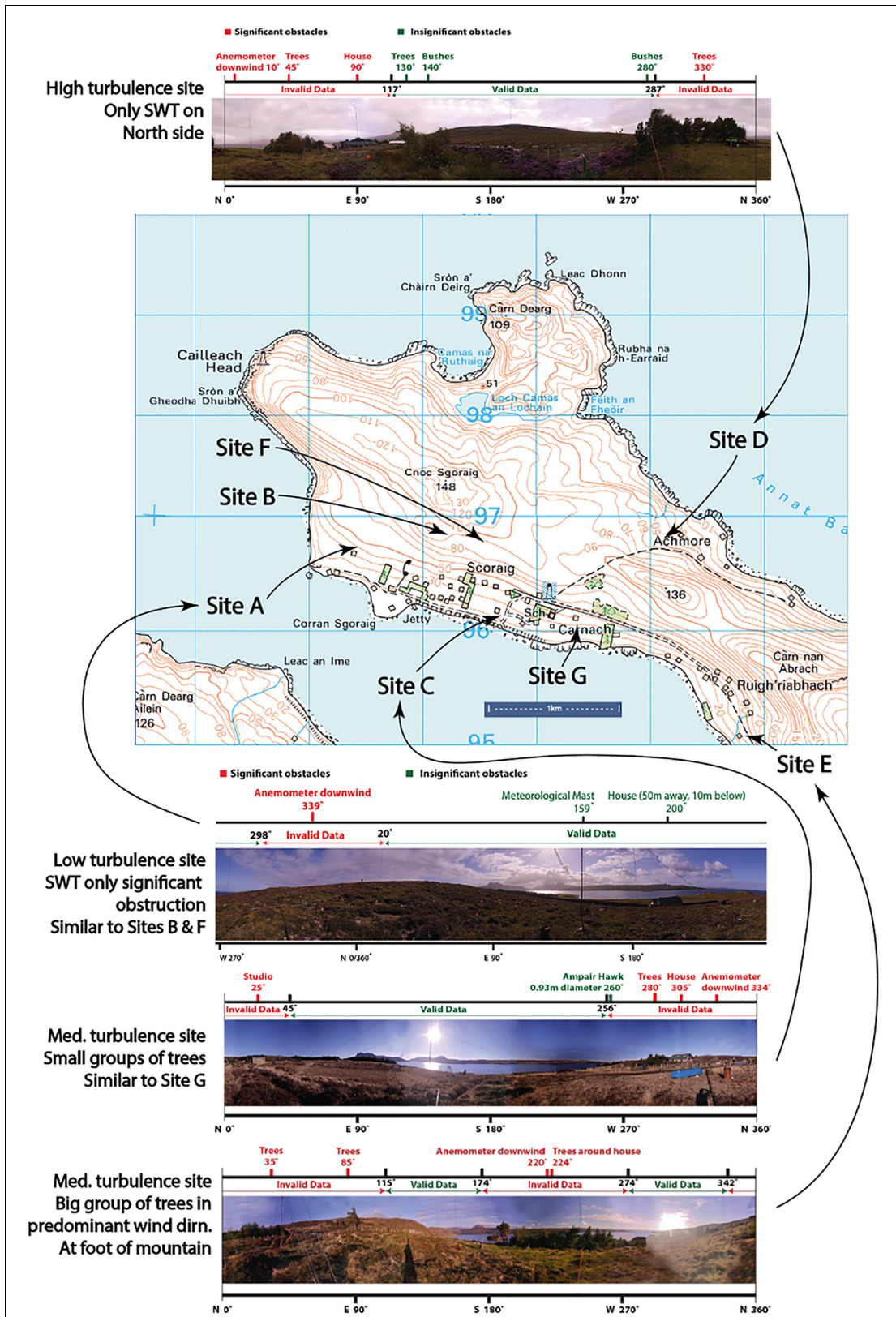


Figure 3. Map showing the location of the seven different test sites featured in this measurement campaign. Photo panoramas taken at the base of the tower of four of the sites show the range of terrain and surrounding obstacles, indicating which sectors were excluded from the analysis. Base map courtesy of Streetmap.co.uk.

Table 5. Specification for the seven turbines tested during this measurement campaign.

	Model	Blades	Generator	Furling	Years in service and major repairs	Significant mods.
A	1.8 N	-Slightly worn leading edges -Chord ok, thickness and setting angles few degrees off, one in negative pitch -Siberian Larch -1.8 m	-12 V -29 mm air gap ^a -Six coils -2x 8-pole NdFeB magnet rotors	-38 Nm tail mom. weight -20° tail hinge angle -0.4 m ² tail area	Installed 2009. Diode replaced.	Magnets on BOTH rotor discs ^b
B	2.4 N	-Leading edges recently completely rebuilt with epoxy -Thickness, chord and setting angle ok -Siberian Larch -2.4 m	-24 V -22.5 mm air gap -Nine coils -2x 12-pole NdFeB magnet rotors	-84 Nm tail mom. weight -20° tail hinge angle -0.72 m ² tail area	Installed 2007. Hub bearings failed (blades and magnet rotors replaced).	Long power cable (183 m)
C	2 F	-Leading edges heavily eroded by the end of testing -Thickness, chord and setting angle ok -Cedar -2 m	-12 V -26 mm air gap -Nine coils -2x 12-pole ferrite magnet rotors	-34 Nm equivalent ^c tail mom. weight -13° tail hinge angle -0.37 m ² tail area	Installed 2013. No failures to date.	Ferrite magnets, new design
D	3 N	-Some cracks and stripped paint -Thickness and chord ok, setting angle distorted -Siberian Larch -3 m	-24 V -20 mm air gap -Nine coils -12-pole dual NdFeB magnet rotors	-88 Nm tail mom. weight -20° tail hinge angle -0.78 m ² tail area	Installed 2009. Dump load failure. Alternator main stud failure. Blades destroyed when hit by tail.	
E	2.4 N	-Leading edges rebuild and repainted -Chord and thickness ok, setting angle slightly off -Siberian Larch -2.4 m	-48 V -19 mm air gap -Nine coils -12-pole dual NdFeB magnet rotors	-63 Nm tail mom. weight -20° tail hinge angle -Tail area unknown	Installed 2008. Tower collapsed, hub bearing replaced, corroded magnets replaced.	Cheap Chinese hub bearing
F	3 N	-Very poor condition, leading edges very worn with lots of splinters -Wide chord, low setting angle, crudely formed triangles glued to roots for better starting performance -Pitch pine -3 m	-24 V -23 mm air gap -Nine coils -12-pole dual NdFeB magnet rotors	-99 Nm tail mom. weight -20° tail hinge angle -Tail area unknown	Installed 2013. Short circuit in tower top junction box.	Long power cable (150 m). Blades very crudely carved by user.

(continued)

Table 5. Continued

Model	Blades	Generator	Furling	Years in service and major repairs	Significant mods.
G-I	2.4 N -Paint completely stripped off one blade -Chord and thickness ok, setting angle several degrees out at tip (one warped into negative pitch) -Siberian Larch -2.4 m	-12 V -20 mm air gap -Nine coils -12-pole dual NdFeB magnet rotors	-48 Nm tail mom. weight -20° tail hinge angle -Tail area unknown	Installed 2011. Short circuit due to trapped wire a week after installation. Tower bent in half. ^d Melted fuse on charge controller.	<i>Jerry-rigged</i> ^e and short tail boom. Blocking diode installed.
G-II	2.4 N -Freshly repainted -Negative pitch blade corrected -Rest as above	-24 V -23.5 mm air gap -Nine coils -12-pole dual NdFeB magnet rotors	-55 Nm tail mom. weight -Rest as above	Tail boom lengthened, stator switched for 24 V delta, blades repainted.	Blocking diode still in place.

^aInternal magnet face to magnet face. Stator designed to be 12 mm thick.

^bStator cast too thick, so not cutting in at low enough wind speeds and not possible to increase flux by decreasing air gap as minimum gap width for mechanical reliability already reached. Increased flux in generator by adding magnets onto second rotor disc.

^cThe tail hinge angle is only 13°. The moment of weight is 52 Nm, but with this tail angle it corresponds to only 34 Nm when comparing to a SWT with a 20° hinge angle. The smaller hinge angle allows a big, strong, long tail with a large vane (0.45 m² design) while not overdoing the tail furling moment.

^dGuys were too steep and top guys not tight plus unusual turbulence from high trees by shoreline. Therefore, 6 m tower upgraded to current 13.5 m tower.

^eIEC 61400-12-1 specifies ±2.5%.

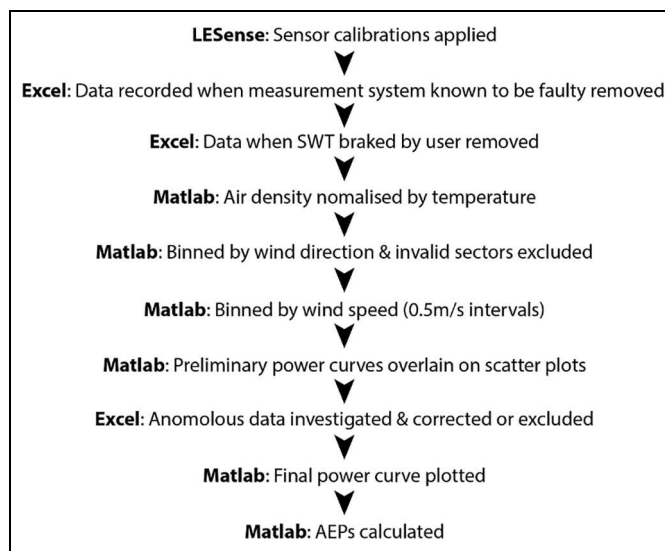


Figure 4. Flow chart showing how the data were processed from the .csv files downloaded from the LeSense into the IEC-61400-12-1 specified performance data using Excel and MATLAB.

Table 6. Comparison of the data sets obtained for each of the seven turbines during this measurement campaign.

Data set	Measurement period	Additional excluded data	No. valid data points	Additional corrected data	Mean wind speed of valid data (m/s)	Max. complete wind speed bin (m/s)
A	131 days	Wind vane stuck; interference on RPM; 0°–19°, 299°–360° (anem. downwind)	14,016		5.46	20.5
B	102 days	357°–360°, 0°–64° (nearby SWT), 100°–151° (anem. downwind)	9184		5.96	18.0
C	60 days	Anemometer disconnected; datalogger disconnected; 256°–360°, 0°–45° (trees, house, anem. downwind)	1764	Current sensor loops calibration error corrected	6.91	19.5
D	94 days	All data from boom-mounted system; 0°–117°, 287°–360° (trees, house and anem. downwind)	5729	Current sensor floating ground re-zeroed	5.31	17.0
E	115 days	Tower collapse; 342°–360°, 0°–115° (trees); 174°–274° (trees, house and anem. downwind)	4882		3.15	13.5
F	37 days	Datalogger battery flat; short circuit in junction box; >28 V (suspected sensor calibration error); 97°–173° (anem. downwind)	2374	Wind vane recalibrated after slipping	8.91	20.0
G-I	106 days	Met mast collapse; RPM sensor failure; 140°–320° (trees and anem. downwind)	4234	Wind vane recalibrated after slipping	3.94	12.0
G-II	61 days	140°–320° (trees and anem. downwind)	3119		2.95	16.5

SWT: small wind turbine; RPM: revolutions per minute.

Other researchers have found that substantial variation between hand carved blades has limited power performance and propose using copy routers to increase the uniformity of blade carving (Clausen et al., 2009; Peterson and Clausen, 2004). However, in this study, the SWTs with least consistent blades were not the worst performing, suggesting that inconsistent blade carving is not the most significant cause of reduced power performance among

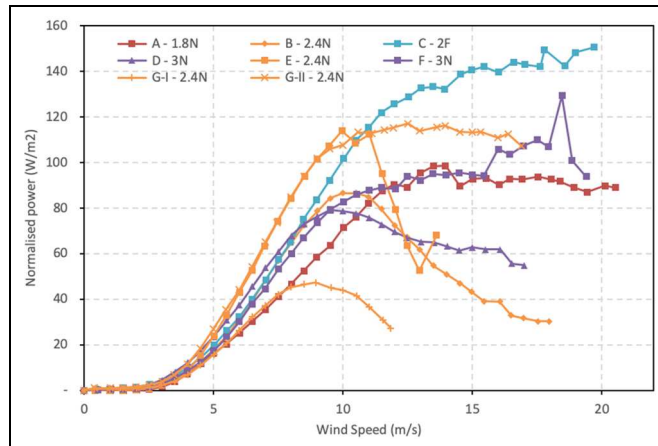


Figure 5. Comparison of normalised power curves measured during this study.

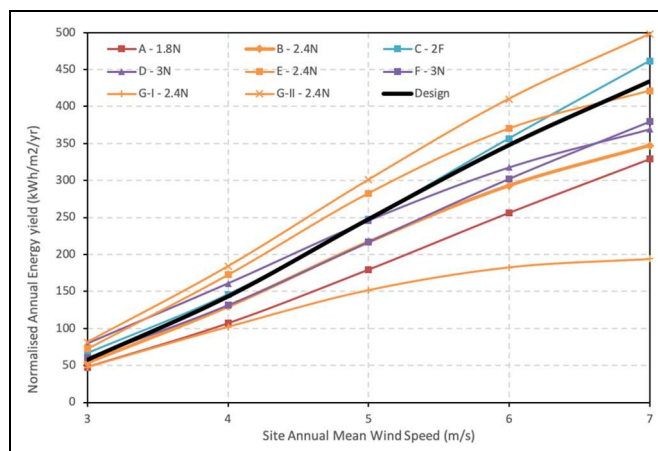


Figure 6. Comparison of normalised annual energy yields from measured data to design values from Piggott's Recipe Book (Piggott, 2013).

this set of SWTs. Of course, successful hand carving not only depends on the skill of the carver but also on the quality of the instructions they are given. Piggott selected aerodynamic profiles that were achievable for hand manufacture (simple to carve and with aerodynamic performance relatively insensitive to small deviations in shape). The results suggest that sufficient detail is given in Piggott's *Recipe Books* for relatively inexperienced users to produce blades of satisfactory quality.

However, anecdotal evidence following the measurement campaign suggests that material selection and maintenance frequency are significant factors. After the power curve testing on Turbine C had been completed, it did not receive any maintenance for 3–4 years and its soft cedar blades lost 10–15 mm off the leading edge. The turbine was struggling to produce power, so the leading edges were rebuilt with epoxy, which was able to restore the machine's ability to produce its rated power. Siberian larch is the standard material for machines on the Scoraig Peninsula, as it's much harder, and preventive maintenance usually takes place annually.

The wide variation of tip speed ratio is a design challenge for direct coupled turbines that work at near-constant voltage, such as Piggott's 'Recipe Book' machines. At high tip speed ratios (typically seen at start-up), flatter, pointier and/or straighter aerofoils with lower drag can enhance power performance. However, at low tip speed ratios (typically when the wind rises above 6 m/s on a low battery voltage and the alternator is running too slow to keep up), wider, more rounded and/or more curved aerofoils are needed to keep the flow attached at high angles of attack and prevent stalling. Hosman (2012) and Monteiro et al. (2013) compared wind tunnel data with Blade Element Momentum (BEM) models of blades carved by hand to Piggott's specification and found that despite the

compromises made to simplify the manufacturing process, the hand carved aerofoils are able to operate over a relatively wide range of angles of attack without stalling. Blade performance is linked to rotational speed, which is proportional to voltage, which varies with both the state of charge of the batteries and the voltage drop in the power cable. Full batteries and high-resistance power cables push up the voltage at the generator, which causes the blades to run faster. For fixed pitch machines, such as these, higher voltage in high winds increases conversion efficiency (measured at the turbine), as internal copper losses are lower, and blade speed rises with wind speed, maintaining optimum tip speed ratio (Monteiro et al., 2013). Conversely, previous datalogging experience (not presented here for brevity) suggested that lower battery voltage might give increased power performance around cut in. To explore this relationship, data collected during this study were binned by voltage to plot separate power curves for each machine; however, only very minimal correlation between voltage and power performance was observed.

The SWT on Site G was upgraded from the worst performing to the best, with voltage drops in the diodes likely to have been a major contributing factor. This machine had a blocking diode installed, as a short circuit in the tower had previously drained the batteries. It originally had a 12 V *Jerry-rigged* stator, which was upgraded to a standard *Recipe Book* 24 V delta-connected stator. The independently rectified *Jerry-rigged* stator has 50% higher internal resistance at low power output, and although the blocking diode was in place when both data sets G-I and G-II were recorded, it would have had twice as much effect at 12 V as it does at 24 V.⁸ As a general trend, the 24 V machines (B, D, F, G-II) outperform the 12 V (A, C, G-I) machines; however, the only 48 V machine (E) sits at the middle of the pack.

Furling. Above 8 m/s, Figure 5 shows that the furling system becomes the dominant influence on the power performance of the wind turbine. Furling systems are designed to be simple and robust, but not necessarily precise. Furling behaviour is designed to regulate output at the rated power, but instantaneous power peaks will be much higher on Piggott's *Recipe Book* machines, as the Axial Flux Permanent Magnet (AFPM) topology is not laminated.⁹ Pitch control systems, (e.g. Proven/Kingspan), tend to be much more consistent in output. They offer better energy yields in high winds, but this is rarely important for battery charging systems as this is when the battery is usually full and the excess power is therefore dumped. Overall, they are much better control systems, but generally have more maintenance and are more costly.

The furling system of the *Recipe Book* turbines is driven by the wind thrust on the blade rotor. In the simplest analysis, this thrust is aligned with the rotor axis, which is offset from the machine's yaw axis. The combination of thrust and offset give rise to a furling moment about the yaw axis that is always present to some degree but rises with approximately the square of wind speed in the simplest case.

The purpose of the tail of the machine is to face the machine into the wind; however, in winds below rated wind speed, it must also counter the furling moment created by the offset thrust. It must therefore have sufficient moment of vane area to create a counter moment using lift and drag forces. The line of the boom at rest (seen from above) is not square to the rotor disc, but angled 20° counter to the offset in an attempt to keep the blade rotor axis roughly aligned to the wind until furling is desired.

As the thrust grows, so does the counter moment exerted by the tail, so the machine remains in equilibrium, as each is roughly proportionate to the square of wind speed. At a certain point, the tail should yield and allow furling. The tail hinge acts as a limiting factor on the counter moment, allowing the machine to furl at a certain wind speed, where the furling moment exceeds this limit, and the tail swings upwards on its hinge. The limit to the counter moment can be controlled using the angle of the tail hinge and the moment of weight of the tail itself.¹⁰

Once the machine starts to yaw, it loses some thrust, and a balance should be found where the wind thrust is limited to the optimum value. The extent to which it needs to rise depends on the wind speed, but the system acts to maintain a roughly constant thrust. In reality, this is a very simplistic analysis because blade rotor aerodynamics in yaw result in a complex array of forces and moments, making furling behaviour very difficult to predict.

Ideally, this limiting moment at which the tail yields and allows the turbine to swing away from the wind should be constant through the full range of the tail movement, but the *Recipe Book* machines use a simple fixed tail hinge axis, so the actual limit to the tail counter moment about a vertical axis is a sinusoidal function of the tail position angle. When the tail hinge is mounted correctly as seen from above, with equal side angle and back angle of the hinge axis, the slope at which the tail rises will increase to a maximum and decrease again over its approximately 90° of travel. It reaches its highest value around midway where the tail is rising most steeply.

The power curve of the machine can be adjusted in the field by adding weight to the tail, so as to increase its moment of weight and thereby delay furling to expose the machine to higher thrust and power. Removing weight

is more difficult as this tends to reduce the strength, length or the area of the tail, which can be detrimental to low wind performance. Using thinner plywood in the vane is probably the best way to reduce power output where the power curve continues to rise above rated power.

The power curves on Figure 5 can be classified into three groups: *rising*, *steady* and *falling*. The tail moment of weight was normalised by the size of the machine, represented by its swept area. An average was taken for each group to determine if this was the defining factor:

1. *Rising* – power performance continues to increase. Normalised tail moment of weight: 9.6 N/m² average (C – 8.5 N/m²; F – 10.8 N/m²).
2. *Steady* – power performance stabilises. Normalised tail moment of weight: 10.6 N/m² average (A–11.7 N/m²; G-II – 9.5 N/m²).
3. *Falling* – power performance falls dramatically. Normalised tail moment of weight: 10.9 N/m² average (B – 14.6 N/m²; D – 9.8 N/m²; E – 10.9 N/m²; G-I – 8.3 N/m²).

While the normalised tail moment of weight was expected to be the key defining factor, there are clearly others in play. In particular, SWT C has one of the lightest normalised tail moments of weight; however, it produced a ‘rising’ power curve. In fact, the moment of weight was measured as 52 Nm; however, this machine was built with a 13° tail angle, which corresponds to an equivalent of 34 Nm compared to the other machines, which are all built with a 20° tail angle. The reason for the smaller hinge angle is to allow a big, strong, long tail with large vane (0.4 m²) while not overdoing the tail furling moment. SWT B is also surprising, as it has a heavy tail, but exhibits a ‘falling’ power curve.

Unintentional variations in the furling hinge angle may have directed the thrust force produced by the tail moment of weight in different directions. A fixed value is given as a design parameter in the *Recipe Book*, so it was assumed to be constant and not measured during this study. However, previous experimentation has shown that the shape of the power curve depends on the balance between the ‘side angle’ and ‘back angle’ of the furling hinge. An angle of 55° (seen from above) is specified in the *Recipe Book* to balance the *side angle* and *back angle*. If the tail hinge projects too far to the side, then the tail will have difficulty starting to lift, which should cause the power curve to peak and then fall as the tail rises more easily towards *top dead centre* on the reduced *back angle*. In contrast, if the tail hinge projects backwards, then the curve will continue to rise as the tail encounters greater resistance as it rises further, forcing the blades to work harder.

Tower lean, the vertical component of wind velocity and turbulence were also suspected to have had a significant influence on the furling performance of these machines. Turbulence is a complex phenomenon, and many studies have highlighted it as a key determinant of SWT power performance (Anup et al., 2019; Battisti et al., 2018; Encraft, 2009; Evans et al., 2017; Trivellato et al., 2012). On Site D, two clear power curves were observed (see Figure 7), both *rising* and *falling*. However, as the *rising* curve was only observed in invalid sectors, the final power curve was *falling*. These sectors were considered invalid partly not only because the anemometer was downwind of the SWT but also because the turbulence from the trees and house could have affected the SWT and anemometer differently (see Figure 2). However, much of the wind in the valid sectors had come over the hill. Although this did not require excluding or correcting under IEC-61400-12-1, as the hill was far away, it clearly created significant turbulence at a much longer length scale which could have had a different effect on furling behaviour. Trivellato et al. (2012) came to a similar conclusion; finding turbulence of varying intensity and length scales can significantly alter power performance, even with a measurement procedure fully compliant with IEC-61400-12-1. Tower lean was also suspected of having a significant influence on the first data set recorded at this site.¹¹ A lean of just 1° creates a 2° difference in the effective tail angle. While this may be insignificant for normal power production, it increases/decreases the effective tail moment of weight in these opposing directions, causing the furling system to activate later in one and earlier in the other. What is more, this effect could have been further magnified, as the wind in the invalid sectors was generally coming uphill, while that in the valid sectors was generally coming downhill. The same trend of rising power curves in uphill winds was also observed on Site F, but further research is needed to establish whether it really is a significant factor in furling behaviour.

Hysteresis was also observed in the power output during furling at Site D, with a higher power output in increasing wind speeds. The cause of this was never fully determined, but it could have been due to excessive friction in the tail bearing causing the rotor to remain at a more acute furling angle during decreasing wind speeds (i.e. sticking at the angle of the previous, higher wind speed), therefore reducing power output. It could also have been due to increased ohmic losses in decreasing wind speed due to the generator having heated up after operating at rated power for a significant period of time.

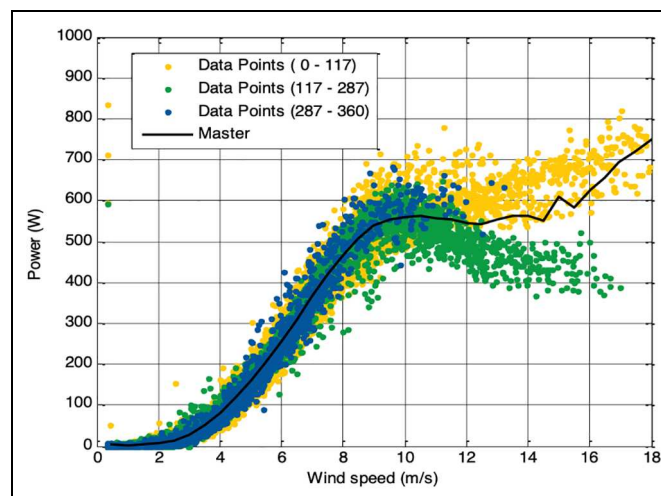


Figure 7. Scatter plot showing the influence of wind direction on furling performance at Site D. Data from the sectors 0° – 117° and 287° – 360° were excluded according to IEC-61400-12-1.

Generic power curves

Figure 8 shows a set of generic power curves produced by non-dimensionalising and averaging the seven *Recipe Book* power curves¹² measured during this study. The upper- and lower-bound curves create an envelope either side of the average curves to indicate the range within which machines that over- or underperform are likely to fall within. The size of this envelope was defined by the variation observed in the individual machines measured during this campaign. In the pre-furling region (< 8 m/s), this was defined by a fixed ratio to the average curve: $\pm 40\%$. Offset errors in current sensors were suspected to have created the artefact of power seemingly being generated at very low wind speeds. As these values exceeded the Betz limit, all curves were set to 0 W below 2 m/s.

Figure 5 shows that extending the $\pm 40\%$ rule into the furling region (> 8 m/s) is not valid due to the unpredictability of furling mechanisms. Consequently, the average curve is levelled off at the crest (91 W/m^2 above 10 m/s) and the upper- and lower-bound curves are defined by the outer envelope around the curves measured during this study. The validity of this technique is tested by also plotting the other power curves obtained during the literature review on Figure 8. In fact, only five curves sit outside the upper/lower bounds:

- Three of COMET-ME's bigger machines lie suspiciously close to Betz limit (likely due to the data from when the anemometer was downwind not being filtered out);
- The 2.4 N measured at Schoondijke juts out below the lower bound due to the unexplained dip in its power curve around 7 m/s;¹³
- The SP-100 1.7 m SWT, which came with no description of the measurement procedure and was an early prototype produced by Soluciones Prácticas.¹⁴

This set of three generic curves (average, upper and lower bound) is intended for use in renewable energy system modelling. The average curve represents a generic Piggott turbine on an average site and should be used as the default input for techno-economic modelling software, such as HOMER. The upper bound represents a well-tuned SWT on a favourable site optimised for maximum power and energy production. The lower bound represents a poorly tuned SWT on a challenging site optimised for maximum reliability. As a general trend, Figure 8 shows that bigger, more sophisticated machines are likely to tend towards the upper bound, while smaller, simpler machines likely to tend towards the lower bound.

Finally, the AEPs of the generic, upper- and lower-bound curves shown in Figure 8 were calculated for sites with a range of mean wind speeds to compare with the normalised design AEPs from Piggott's (2013) *Recipe Book*. Figure 9 shows Piggott's design values to be relatively accurate, slightly underpredicting on low wind sites (up to -20%) and slightly overpredicting in medium to high wind sites (up to $+5\%$). However, the upper and lower bounds show that actual energy yields of any individual machine could vary from the generic values by up to

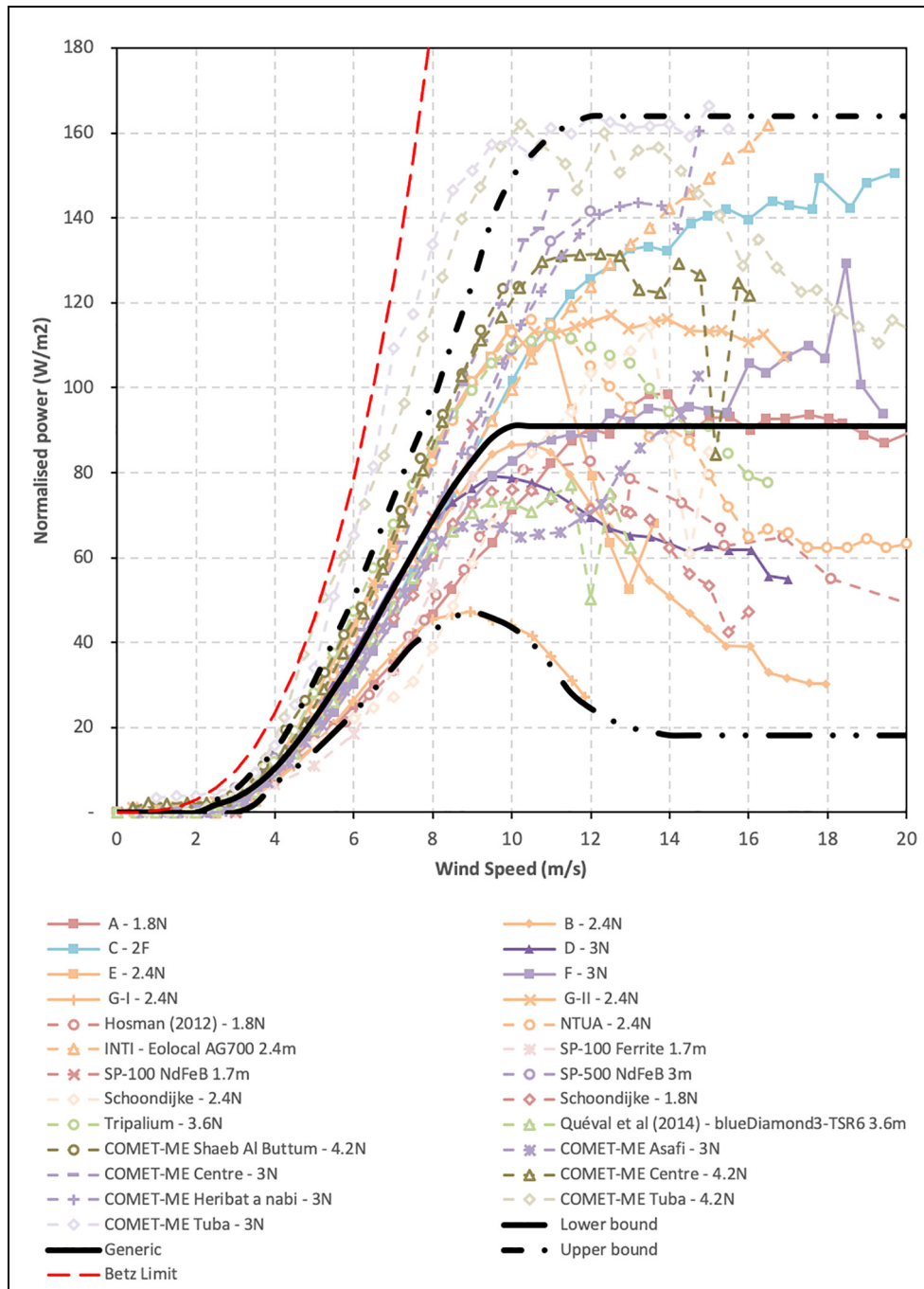


Figure 8. Montage of all *Recipe Book* power curves measured during this study with those reported in the literature. Overlaid is a generic curve, with an upper and lower bound surrounding the range of measured performance curves.

$\pm 42\%$ on low wind sites to $+ 57/-51\%$ on high wind sites. Relative to Piggott’s design values, this becomes $+ 70/-31\%$ on low wind sites and $+ 57/-51\%$ on high wind sites.

Conclusion and recommendations for further work

This article concludes that unlike the machines measured during the infamous Warwick Trials, Piggott’s estimates for the annual energy yields of his *Recipe Book* machines are an accurate prediction of their average real-world

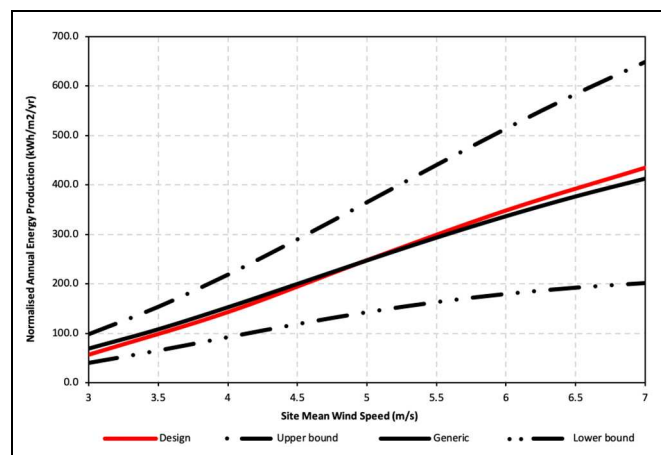


Figure 9. Comparison of design AEP predictions from Piggott's *Recipe Book* with the empirical generic and upper-/lower-bound curves generated from the seven SWTs measured during this study.

performance (+ 5/−20%). However, the performance of individual machines can be significantly above or below this (+ 70/−51%). These deviations are sometimes intentional, where reliability is prioritised over power performance, but often unintentional.

These unintentional deviations can result in improperly designed renewable energy systems. For underperforming systems, disappointing energy yields can result in user dissatisfaction and premature battery failure or additional expenditure other power sources. For overperforming systems, users may be pleasantly surprised; however, a lot of the additional energy is likely to go back to nature through the dump load and they could have purchased a smaller and cheaper SWT. There is also the risk that the increased power could overload other system components, especially for machines with a heavy furling system and 'rising' power curve.

The following recommendations can prevent and mitigate the impact of under- or overperforming SWTs:

Feasibility:

- Update the *Recipe Book*: Give an indication of the range of AEPs and a list of factors users can look for on underperforming machines.
- Techno-economic modelling inputs: The average generic curve should be used as the default power curve for Piggott turbines in techno-economic modelling software, such as HOMER. However, the upper- and lower-bound curves can also be useful for performing sensitivity analyses.
- Hybridise: Leverage the predictability of solar by including PV at the design stage, especially when the two resources complement each other, daily and/or seasonally.

Manufacture:

- Mounting frame: Achieve 'steady' furling behaviour by paying particular attention to the hinge angle to ensure 'side angle' and 'back angle' are balanced.

Installation:

- Optimise each SWT for its site and user: The challenges experienced during this study are testament to the fact there are many intertwined factors that govern real-world furling performance. Making a furling system heavier or rewelding the tail hinge with more *back angle* should turn a *falling* power curve into a *rising* one and finding the sweet spot for the air gap should increase the power produced at any point on the power curve. These modifications are suitable for low wind, low turbulence and/or easily accessible sites; users who prioritise power production in high winds over reliability; and/or turbines that will receive regular preventive maintenance. Vice versa equally applies.

Operation and Maintenance:

- Post-installation monitoring and fine-tuning: Each small wind system should receive regular attention to ensure it is performing as expected. This can be determined by monitoring the SWT's performance using any available tools, from simple observations of the SWT's behaviour in different wind conditions to

physical measurements. Wind Empowerment's Maintenance Manual (Cesa et al., 2018) can help pinpoint the underlying cause of poorly performing SWTs and guide the reader through appropriate remedial action. As this study illustrates, comparing performance between machines is difficult, but taking before and after measurements on a particular machine to assess the effect of a modification is much easier. Carrying out a measurement campaign as detailed as this study would be impractical in most cases. Fortunately, there are several more practical options:

- Power/energy measurements:
- Many inverters, charge controllers and system management devices already record energy yields, so simply writing these down and comparing with average wind speeds over the same time periods can give an indication of SWT performance.
- A simple clamp meter can be used to manually record instantaneous current and voltage data. Recording data every 10 s for several hours during a storm could be a laborious, but very quick and low cost means of obtaining enough data to construct a simple power curve.
 - Wind speed measurements:
 - Include a simple boom-mounted anemometer on each turbine at installation and record data using a low-cost datalogger.
 - Wind speed data from a nearby anemometer may give an indication of the wind speed at the turbine; however, the accuracy of this method is likely to be low in complex terrain, especially if the anemometer is far off hub height ($> \pm 25\%$) or when the anemometer is far away from the turbine (> 100 m).

While this study had hoped to identify and quantify the impact of a range of different factors on power performance, in practice, it was extremely challenging to disentangle the multitude of different factors in play. Each power curve that was measured offered a snapshot of that machine at that moment in time; however, much more could have been learned by taking remedial action on each turbine and then remeasuring the power curve. By changing just one variable at a time, the impact of that particular variable on power performance could be isolated and quantified. This approach was trialled with the final turbine measured during this study (G), which transformed it from the worst performing machine into the best and increasing energy yields by up to 156%. However, as multiple factors were changed at once, it was not possible to pinpoint exactly which factor had the greatest effect.

This approach could be facilitated by developing a mobile power curve testing kit. This could be rotated around different turbines, testing first at installation, after 6 months and then approximately every 2 years. If performance is worse than expected, remedial action could be taken and the power curve re-measured. This could be similar in form to the set up used in this study; however, by combining the practical techniques listed above, it could become a valuable tool for post-installation performance verification and optimisation by making it cheaper, simpler and quicker to set up, record and analyse the data.

Acknowledgements

The authors thank the seven households that invited them into their homes to install the equipment needed to take the measurements described in this study. Their willingness to openly discuss the behaviour of the machines under test and assist with setting up, monitoring and dismantling the test equipment not only made this study much easier but also much more enjoyable. They also thank the members of the Wind Empowerment association, who provided valuable guidance throughout the course of this study.

Declaration of conflicting interests

The author(s) declared no potential conflicts of interest with respect to the research, authorship, and/or publication of this article.

Funding

The author(s) disclosed receipt of the following financial support for the research, authorship, and/or publication of this article: This work was supported through a PhD scholarship at the E-Futures DTC (EP/G037477/1) and Doctoral Prize Fellowship (EP/L505055/1), both administered by the EPSRC at the University of Sheffield, UK.

Credit author statement

Jon Leary: conceptualisation, methodology, investigation, formal analysis, writing – original draft, visualisation, funding acquisition. Hugh Piggott: conceptualisation, methodology, investigation, formal analysis, resources, writing – review and editing, supervision. Robert Howell: writing – review and editing, supervision.

Data availability

Underlying research data are available on request.

ORCID iD

Jon Leary  <https://orcid.org/0000-0002-8832-416X>

Notes

- Both curves have an unexplained dip around 7 m/s, which is particularly pronounced for the 2.4 m machine (see Figure 8), indicating that there may be underlying issues with the measurement procedure.
- A non-profit organisation closely associated with the Mechanical Engineering Department of the University of Coimbra.
- IEC 61400-12-1 states that for SWTs, data should be averaged at 1-min intervals; however, the LeNet device was only capable of averaging at 10-min intervals. Standard deviations and maximum values during the 10-min intervals were recorded for the wind speed and rotational speed sensors, as per IEC 61400-12-1; however, the LeNet was only capable of recording means for all other inputs.
- Wider air gap prevents mechanical contact between rotor and stator, while thinner air gap offers higher flux density.
- Heavier tails furl at higher wind speeds, offering increased power performance, while lighter tails furl at lower wind speeds, protecting the machine from higher winds when the batteries are likely to be full anyway.
- Each winding rectified separately – no delta connection between phases.
- Data set G-I is presented alongside the results for the other six SWTs; however, only data set G-II was used to calculate the generic power curve for Recipe Book machines.
- The rectifier already puts two diodes in series, which with the blocker makes three, making up a total of about 2 volts or approximately 15% loss in the 12 V case, but half of that for 24 V.
- Alternators with laminated cores are self-limiting, (e.g. African Wind Power, Bergey or Whisper SWTs or those built with car alternators) as they have high internal impedance, so cannot produce power peaks, but instead overspeed. As this impedance is reactive, it does not imply large copper losses; however, overspeeding increases wear and can alter furling behaviour by making the rotor 'seek the wind' in a vicious circle that can be very destructive.
- Consider the analogy of pushing a trolley up a ramp. The horizontal force required to do this depends on the weight of the trolley and the steepness of the ramp. Here, we deal with moments rather than forces, but the analogy should help with visualisation.
- This initial data set was subsequently disregarded due to use of boom-mounted anemometer, interference from logger battery charger on RPM sensor and high wind shear on the low tower. These problems were addressed by installing a separate met mast, relocating the battery charger and installing a taller SWT tower.
- That is, data sets A-F and G-II, excluding G-I as it was not a *Recipe Book* machine.
- This curve was measured using a single anemometer for an entire row of SWTs.
- Magnets were upgraded from ferrite to neodymium, but other modifications may also have taken place simultaneously.

References

- Anup KC, Whale J and Urmee T (2019) Urban wind conditions and small wind turbines in the built environment: A review. *Renewable Energy* 131: 268–283.
- Batchelor S, Scott N, Daoqi L, et al. (1999) *Evaluating the impact of wind generators in inner Mongolia. Project Technical Report*, DfID, Gamos Ltd, Reading. Available at: <http://www.gamos.org/research-and-publications-mainmenu-26/project-documents/evaluating-the-impact-of-wind-generators-in-inner-mongolia-technical-report/download>
- Battisti L, Benini E, Brighenti A, et al. (2018) Small wind turbine effectiveness in the urban environment. *Renewable Energy* 129: 102–113.
- blueEnergy (2009) *Technical Report – 12' Turbine Final Design*. Bluefields: blueEnergy.
- Carvalho Neves P, Gleditsch M, Bennet C, et al. (2015) Assessment of locally manufactured small wind turbines as an appropriate technology for the electrification of the Caribbean Coast of Nicaragua. *AIMS Energy* 3(1): 41–74.
- Cesa G, Brunel M-L and Strasilla J (2018) *Maintenance manual for 'Piggott' small wind turbines. Wind Empowerment*. Available at: <http://windempowerment.org/maintenance-working-group/>
- Chiroque J, Sánchez T and Dávila C (2008) *Microaerogeneradores de 100 y 500 W. Modelos IT-PE-100 y SP -500*. Lima: Soluciones Prácticas. Available at: <http://www.solucionespracticas.org.pe/publicaciones/pdf/Microaerogeneradores>

- Clausen PD, Freere P, Peterson P, et al. (2009) The shape and performance of hand-carved small wind turbine blades. *Wind Engineering* 33(3): 229–304.
- Dotan N (2017) COMET-ME power curves. Available at: <https://comet-me.org/>
- Eales A, Sumanik-Leary J and Latoufis K (2016) *Market assessment for locally manufactured small wind turbines in Ethiopia. Wind Empowerment and Mercy Corps*. Available at: <http://windempowerment.org/market-assesment-working-group/>
- Encraft (2009) *Warwick wind trials project final report*. Available at: <https://www.warwickwindtrials.org.uk/>
- Evans SP, Anup KC, Bradney DR, et al. (2017) The suitability of the IEC 61400-2 wind model for small wind turbines operating in the built environment. *Renewable Energy and Environmental Sustainability* 2: 31.
- Ferrer-Martí L, Garwood A, Chiroque J, et al. (2010) A community small-scale wind generation project in Peru. *Wind Engineering* 34(3): 277–288.
- Ghimire P, Sharma R, Lamichhane C, et al. (2010) Kathmandu alternative power and energy group: Our experience in promotion of low cost wind energy technology in Nepal. *Wind Engineering* 34(3): 313–324.
- Hosman N (2012) *Performance Analysis and Improvement of a Small Locally Produced Wind Turbine for Developing Countries*. Delft: TU Delft.
- Ingreenious (2010) *Small Wind PV-Curves Schoondijke*. Schoondijke, The Netherlands. Available at: http://www.microwindturbine.be/Rapportering_files/PvCurvesZeeland.pdf
- INTI (2016) *Observación de Funcionamiento Eolocal AG700: Verificación de estado con dos meses de funcionamiento*. Neuquén: INTI.
- Latoufis K, Gravas A, Messinis G, et al. (2014) Locally manufactured open source hardware small wind turbines for rural electrification. *Boiling Point* 38–41. Available at: <http://www.hedon.info/BP62>
- Latoufis K, Kotsampopoulos P, Hatzigiorgiou N, et al. (2012) Axial flux permanent magnet generator design for low cost manufacturing of small wind turbines. *Wind Engineering* 36(4): 411–432.
- Latoufis KC, Pazios TV and Hatzigiorgiou ND (2015) Empowering communities for sustainable rural electrification. *IEEE Electrification Magazine* 3(1): 68–78.
- Leary J, Howell R, While A, et al. (2012) Post-installation analysis of locally manufactured small wind turbines: Case studies in Peru. In: *2012 IEEE third international conference on sustainable energy technologies (ICSET)*, Kathmandu, 24–27 September, pp. 396–401. Singapore: IEEE.
- Leary J, Schaub P and Clementi L (2019) Rural electrification with household wind systems in remote high wind regions. *Energy for Sustainable Development* 52: 154–175.
- Leary J, To LS and Alsop A (2018) *Is There Still a Role for Small Wind in Rural Electrification Programmes?* Loughborough. LCEDN (Low Carbon Energy for Development Network & Wind Empowerment). Available at: www.lcedn.com
- Medd A and Wood DH (2018) Small wind turbine performance assessment for Canada. In: Battisti L and Ricci M (eds) *Wind Energy Exploitation in Urban Environment. Turbwind 2017. Green Energy and Technology*. Cham: Springer, pp. 155–163.
- Monteiro JP, Silvestre MR, Piggott H, et al. (2013) Wind tunnel testing of a horizontal axis wind turbine rotor and comparison with simulations from two Blade Element Momentum codes. *Journal of Wind Engineering and Industrial Aerodynamics* 123: 99–106.
- Peterson P and Clausen PD (2004) Timber for high efficiency small wind turbine blades. *Wind Engineering* 28(1): 87–96.
- Piggott H (2005) *How to Build a Wind Turbine*. Scoraig: Scoraig Wind Electric.
- Piggott H (2009) *A Wind Turbine Recipe Book – 2009 Edition*. Scoraig: Scoraig Wind Electric. Available at: www.scoraigwind.com
- Piggott H (2013) *A Wind Turbine Recipe Book – 2013 Edition*. Scoraig: Scoraig Wind Electric. Available at: www.scoraigwind.com
- Piggott H (2014) *2F Wind Turbine Construction Manual*. Scoraig: Scoraig Wind Electric. Available at: <http://scoraigwind.co.uk/>
- Quéval L, Joulain C and Casillas CE (2014) Measuring the power curve of a small-scale wind turbine: A practical example. In: *Proceedings of the 1st international e-conference on energies*, 14–31 March, Sciforum Electronic Conference Series, vol. 1, id. c011. DOI: 10.3390/ece-1-c011
- Sánchez T, Chiroque JE and Ramírez S (2002) *Evaluación Y Caracterización De Un Aerogenerador De 100w*. Lima: Soluciones Prácticas. Available at: <http://www.solucionespracticas.org.pe>
- SE4All (2017) *GLOBAL TRACKING FRAMEWORK: Progress toward Sustainable Energy*. Washington, DC. Available at: <https://www.seforall.org/>
- Site Expérimental pour le Petit Eolien National (2013) *Rapport de Test n 32.6 du 27/09/2013 – Eolienne auto construite Piggott –1.7 kW*. Malbouissou, France. Available at: <http://afppe.org/wp-content/uploads/2019/11/Rapport-SEPEN-32.6-Eolienne-autoconstruite-Piggott-1.7-kW-Connecte-Reseau.pdf>
- Sumanik-Leary J, While A and Howell R (2013) *Small wind turbines for decentralised rural electrification: Case studies in Peru, Nicaragua and Scotland*. PhD Thesis, University of Sheffield. Available at: <http://etheses.whiterose.ac.uk/6282/>
- Tripalium (2017) *Construire une éolienne*. Valence. Available at: <https://www.tripalium.org/manuel>
- Trivellato F, Battisti L and Miori G (2012) The ideal power curve of small wind turbines from field data. *Journal of Wind Engineering and Industrial Aerodynamics* 107–108: 263–273.